

Magnetic Spin Ladder $(\text{C}_5\text{H}_{12}\text{N})_2\text{CuBr}_4$: High-Field Magnetization and Scaling near Quantum Criticality

B. C. Watson, V. N. Kotov, and M. W. Meisel

Department of Physics and The Center for Condensed Matter Sciences, University of Florida, P.O. Box 118440, Gainesville, Florida 32611-8440

D. W. Hall

National High Magnetic Field Laboratory, Florida State University, Tallahassee, Florida 32310

G. E. Granroth, W. T. Montfrooij, and S. E. Nagler

Oak Ridge National Laboratory, Building 7692, MS 6393, P.O. Box 2008, Oak Ridge, Tennessee 37831

D. A. Jensen, R. Backov, M. A. Petruska, G. E. Fanucci, and D. R. Talham

Department of Chemistry, University of Florida, P.O. Box 117200, Gainesville, Florida 32611-7200
(Received 9 August 2000)

The magnetization, $M(H \leq 30 \text{ T}, 0.7 \leq T \leq 300 \text{ K})$, of $(\text{C}_5\text{H}_{12}\text{N})_2\text{CuBr}_4$ has been used to identify this system as an $S = 1/2$ Heisenberg two-leg ladder in the strong-coupling limit, $J_\perp = 13.3 \text{ K}$ and $J_\parallel = 3.8 \text{ K}$, with $H_{c1} = 6.6 \text{ T}$ and $H_{c2} = 14.6 \text{ T}$. An inflection point in $M(H, T = 0.7 \text{ K})$ at half saturation, $M_s/2$, is described by an effective XXZ chain. The data exhibit universal scaling behavior in the vicinity of H_{c1} and H_{c2} , indicating that the system is near a quantum critical point.

DOI: 10.1103/PhysRevLett.86.5168

PACS numbers: 75.10.Jm, 75.40.Cx, 75.50.Ee, 75.50.Xx

Magnetic spin ladders are a class of low dimensional materials with structural and physical properties between those of 1D chains and 2D planes. In a spin ladder, the vertices possess unpaired spins that interact along the legs via J_\parallel and along the rungs via J_\perp , but are isolated from equivalent sites on adjacent ladders, i.e., interladder $J' \ll J_\parallel, J_\perp$. Recently, a considerable amount of attention has been given to the theoretical and experimental investigation of spin ladder systems as a result of the observation that the microscopic mechanisms in these systems may be related to the ones governing high temperature superconductivity [1,2]. The phase diagram of the antiferromagnetic spin ladder in the presence of a magnetic field is particularly interesting. At $T = 0$ with no external applied field, the ground state is a gapped, disordered quantum spin liquid. At a field H_{c1} , there is a transition to a gapless Luttinger liquid phase, with a further transition at H_{c2} to a fully polarized state. Both H_{c1} and H_{c2} are quantum critical points [2]. Near these points, the magnetization has been predicted to obey a universal scaling function [3], but until now, this behavior has not been observed experimentally.

A number of solid-state materials have been proposed as examples of spin ladder systems, and an extensive set of experiments have been performed on $\text{Cu}_2(\text{C}_5\text{H}_{12}\text{N}_2)_2\text{Cl}_4$, referred to as $\text{Cu}(\text{Hp})\text{Cl}$ [4]. The initial work identified this material as a two-leg $S = 1/2$ spin ladder [4–12]. Although quantum critical behavior has been preliminarily identified in this system near H_{c1} , this assertion is based on the use of scaling parameters identified from the experimental data rather than the ones predicted theoretically [11,12]. Furthermore, more recent work

has debated the appropriate classification of the low temperature properties [13–19]. Clearly, additional physical systems are necessary to experimentally test the predictions of the various theoretical treatments of two-leg $S = 1/2$ spin ladders.

Herein, we report evidence that identifies bis(piperidinium)tetrabromocuprate(II), $(\text{C}_5\text{H}_{12}\text{N})_2\text{CuBr}_4$ [20], hereafter referred to as BPCB, as a two-leg $S = 1/2$ ladder that exists in the strong-coupling limit, $J_\perp/J_\parallel > 1$. High-field, low-temperature magnetization, $M(H \leq 30 \text{ T}, T \geq 0.7 \text{ K})$, data of single crystals and powder samples have been fit to obtain $J_\perp = 13.3 \text{ K}$, $J_\parallel = 3.8 \text{ K}$, and $\Delta \sim 9.5 \text{ K}$, i.e., at the lowest temperatures finite magnetization appears at $H_{c1} = 6.6 \text{ T}$ and saturation is achieved at $H_{c2} = 14.6 \text{ T}$. An unambiguous inflection point in the magnetization, $M(H, T = 0.7 \text{ K})$, and its derivative, dM/dH , is observed at half the saturation magnetization, $M_s/2$. This feature is symmetric about $M_s/2$, consistent with expectations for a simple spin ladder. Any presence of asymmetry, as was observed in $\text{Cu}(\text{Hp})\text{Cl}$ [5–8], most likely arises from other factors. Our $M_s/2$ feature cannot be explained by the presence of additional exchange interactions, e.g., diagonal frustration J_F , but is well described by an effective XXZ chain, onto which the original spin ladder model (for strong coupling) can be mapped in the gapless regime $H_{c1} < H < H_{c2}$ [21]. After determining H_{c1} and with no additional adjustable parameters, the magnetization data are observed to obey a universal scaling function [3]. This observation supports our identification of BPCB as a two-leg $S = 1/2$ Heisenberg spin ladder with $J' \ll J_\parallel$.

The crystal structure of BPCB has been determined to be monoclinic with stacked pairs of $S = 1/2$ Cu^{2+} ions forming magnetic dimer units [20]. The CuBr_4^{-2} tetrahedra are cocrystallized along with the organic piperidinium cations so that the crystal structure resembles a two-leg ladder, Fig. 1. The rungs of the ladder are formed along the c^* axis (19.8° above the c axis and $+23.4^\circ$ away from the a - c plane [20]) by adjacent flattened CuBr_4^{-2} tetrahedra related by a center of inversion. The ladder extends along the a axis with 6.934 \AA between Cu^{2+} spins on the same rung and 8.597 \AA between rungs. The magnetic exchange, J_\perp , between the Cu^{2+} spins on the same rung is mediated by the orbital overlap of Br ions on adjacent Cu sites. The exchange along the legs of the ladder, J_\parallel , is also mediated by somewhat longer nonbonding ($\text{Br}\cdots\text{Br}$) contacts and possibly augmented by hydrogen bonds to the organic cations. A frustrating diagonal exchange, J_F , is possible, although it should be weak ($J_F \ll J_\parallel$), and so the potential of a finite J_F on the short diagonal was considered in our analysis.

Shiny, black crystals of BPCB were prepared by slow evaporation of solvent from a methanol solution of [(pipdH)Br] and CuBr_2 , and milling of the smallest crystals was used to produce the powder samples. The stoichiometry was verified using CHN analysis, and 9 GHz ESR measurements were completely consistent with the previously reported data, i.e., $g(\text{powder}) = 2.13$ [20]. In addition, deuterated specimens were produced and used in neutron scattering studies performed at the HFIR at Oak Ridge National Laboratory. No evidence for long-range magnetic order or structural transitions was observed down to 11 K by powder diffraction and 1.5 K for single crystal diffraction in the $[h\ 0\ 1]$ scattering plane. The low-field magnetic measurements were performed using a SQUID magnetometer. The high-field work was conducted

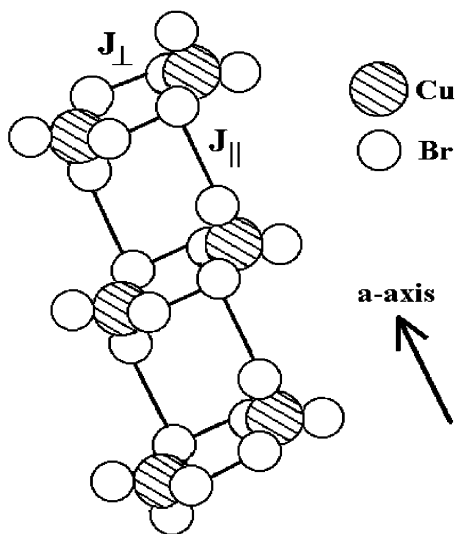


FIG. 1. Schematic of the crystal structure of BPCB. The legs (rungs) are along the a axis (c^* axis); see text.

at the NHMFL using a 30 T, 33 mm bore resistive magnet and a vibrating (82 Hz) sample magnetometer equipped with a Cernox thermometer [22].

The low-field, 0.1 T, magnetic susceptibility, χ , of a powder sample, 166.7 mg, is shown as a function of temperature in Fig. 2. The data from single crystals, with the magnetic field oriented along the a , b , and c axes in separate measurements, are indistinguishable from the results obtained with the powder specimen. The general shape of the curve is typical of low-dimensional magnetic systems, and more specifically, it possesses a rounded peak at $\approx 8 \text{ K}$ and an exponential temperature dependence below the peak. Consistent with the neutron scattering results, no evidence of long-range ordering was observed down to 2 K. A small extrinsic Curie-like impurity contribution ($=1.5\%$ of the total number of Cu spins) and a temperature-independent diamagnetic term ($\chi_{\text{dia}} = -2.84 \times 10^{-4} \text{ emu/mol}$, which is the sum of the core diamagnetism, estimated from Pascal's constants to be $-2.64 \times 10^{-4} \text{ emu/mol}$, and the background contribution of the sample holder) were subtracted from the data in Fig. 2. The Curie-Weiss temperature θ , and the Curie constant C , can be extracted from a fit [$\chi(T) = \chi_{\text{dia}} + C/(T + \theta)$, $50 \text{ K} < T < 300 \text{ K}$], and we find $C = 0.433 \pm 0.002 \text{ emu K/mol}$ and $\theta = 5.3 \pm 0.1 \text{ K}$ [23]. These values are close to $C = 0.425 \text{ emu K/mol}$ ($S = 1/2$, $g = 2.13$) and $\theta \approx (J_\perp + 2J_\parallel)/4 = 5.2 \text{ K}$ [24].

Initially, using exact diagonalization methods with 12 spins, the $\chi(T)$ data were fit to obtain the values $J_\perp = 13.3 \text{ K}$, $J_\parallel = 3.8 \text{ K}$ for a ladder Hamiltonian and

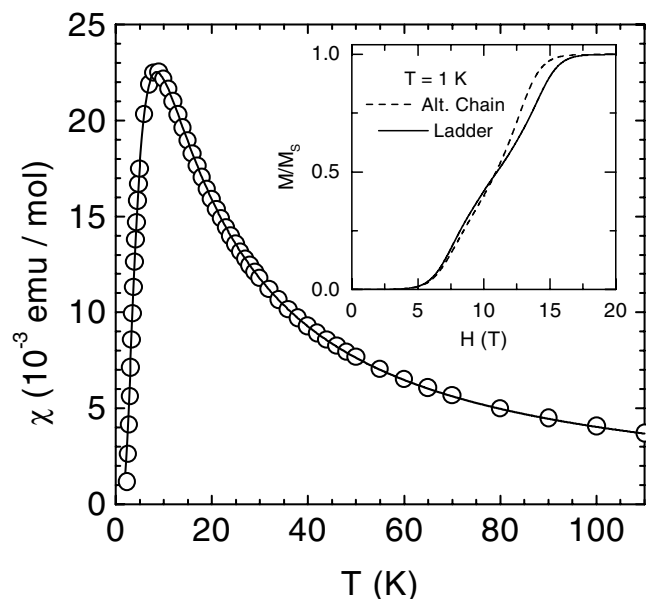


FIG. 2. The $\chi(T)$ of a powder sample (166.7 mg) in 0.1 T. The line is the result of an exact diagonalization of a ladder Hamiltonian with 12 spins when $J_\perp = 13.3 \text{ K}$ and $J_\parallel = 3.8 \text{ K}$; see text. The inset shows the $M(H, T = 1 \text{ K})$ expectations of an exact diagonalization of the alternating chain and ladder Hamiltonians with the exchange values given in the text.

$J_1 = 13.7$ K, $J_2 = 5.3$ K for an alternating chain Hamiltonian. Both fits are indistinguishable from the solid line shown in Fig. 2. Therefore, using only the low-field $\chi(T)$ data, we were unable to distinguish between the ladder and alternating chain models, and this situation was not improved by fitting the $M(H \leq 5$ T, $T = 2$ K) data. However, in extensions up to the saturation magnetization, M_s , the alternating chain model generated $M(H, T < J_{\parallel})$ curves that were asymmetric about $M_s/2$, as reported for Cu(Hp)Cl [8,23], and the spin ladder description predicted symmetric behavior; see Fig. 2 inset. Since our experimental resolution was estimated to be sufficient to allow us to differentiate between the two models, the high magnetic field studies were initiated.

The high-field, $H \leq 30$ T, magnetization of a powder sample, 208.2 mg, is shown in Fig. 3. Since M_s was reached in our studies, we were able to directly measure and subtract a small, temperature-independent contribution ($\chi_{\text{dia}} \approx -2.84 \times 10^{-4}$ emu/mole), which is the same value obtained in our low-field work. Measurements were also made on a single crystal, 18.9 mg, with $H \parallel a$ -axis and for $T \geq 1.6$ K. Within the resolution, the data are the same for the powder and single crystal samples. Furthermore, the data were acquired while ramping the field in both directions, and no hysteresis was observed.

The low energy states of the spin ladder Hamiltonian can be mapped, in the strong-coupling limit, onto the $S = 1/2$ XXZ chain [21], allowing $M(H, T)$ to be modeled. The

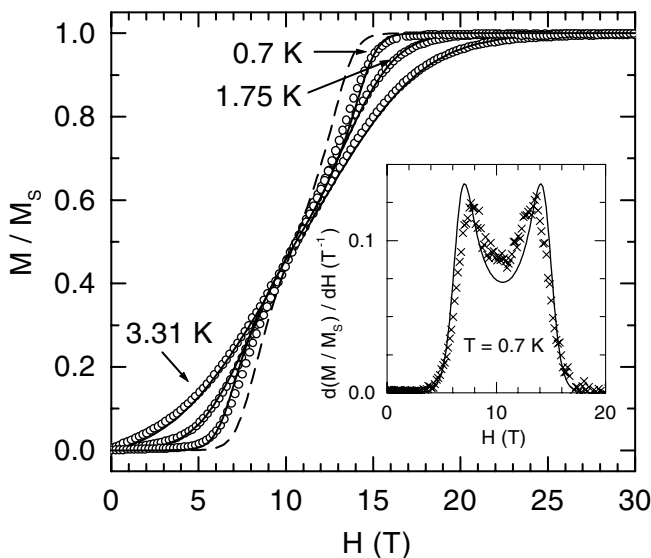


FIG. 3. The normalized magnetization, M/M_s , of a powder sample (208.2 mg). The data traces are limited to ≈ 150 (of ≈ 3000) points for clarity. The lines are spin ladder predictions of an effective XXZ chain when $J_{\perp} = 13.3$ K and $J_{\parallel} = 3.8$ K. At $T = 0.7$ K, the inflection point at $M_s/2$ is clearly visible, and the inset shows the derivative of this data. The dashed line is the alternating chain model prediction for 0.7 K when J_1, J_2 are taken to be the values obtained from fitting the data in Fig. 2; see text.

solid lines in Fig. 3 were obtained by numerical integration of the Bethe ansatz equations for the effective XXZ chain [25], using the parameters describing the spin ladder fit for $\chi(T)$. All of the data, Figs. 2 and 3, are reproduced by one set of exchange values when using the ladder model. On the other hand, the alternating chain model fails to fit all of the data with a single set of parameters. For example, the dashed line in Fig. 3 is $M/M_s(H, T = 0.7$ K) calculated from the alternating chain mapping onto the XXZ chain when $J_1 = 13.7$ K and $J_2 = 5.3$ K, i.e., the values obtain from fitting $\chi(T)$, Fig. 2, by an alternating chain model. In addition, our data were analyzed with a ladder model that also incorporated a frustrating interaction, J_F [26], and we can estimate an upper bound of $J_F < 0.5$ K. Consequently, all of the data are consistent with a strongly coupled ladder description for BPCB, where $J_{\perp} = 13.3 \pm 0.2$ K, and $J_{\parallel} = 3.8 \pm 0.1$ K.

To leading order, $g\mu_B H_{c1} = J_{\perp} - J_{\parallel}$, and $g\mu_B H_{c2} = J_{\perp} + 2J_{\parallel}$ [26,27]. Using the previously mentioned parameters, we obtain $H_{c1} = 6.6$ T and $H_{c2} = 14.6$ T, identical with the experimental results. The inset in Fig. 3 shows the derivative curve, $d(M/M_s)/dH$, of our data at the lowest temperature. The symmetric double bump structure and its evolution with temperature has been studied theoretically [17] but has not been observed previously in $S = 1/2$ two-leg ladder materials. Even though our theoretical curve somewhat overestimates the sharpness of $d(M/M_s)/dH$, the overall agreement between theory and experiment, including the evolution of $M(H, T)$, Fig. 3, is excellent, and involves no adjustable parameters once H_{c1} is defined. Furthermore, the fact that we see only one feature at $M_s/2$ between H_{c1} and H_{c2} is evidence that our strongly interacting dimers are not coupling to form 2D [28] or 3D [29,30] networks.

At H_{c1} , BPCB undergoes a transition from gapped dimer pairs to a gapless Luttinger liquid phase with fermionic excitations, where the magnetization is proportional to the fermion density [3,31,32]. This transition can be described as a condensation of a dilute gas of bosons (dimers), and quasiparticle interactions are irrelevant at the transition point. At H_{c2} , an analogous situation exists where the transition is between the Luttinger liquid and spin polarized phases. When $T, g\mu_B|H - H_{c1}|$, and $g\mu_B|H_{c2} - H|$ are $\lesssim J_{\parallel}$, the 1D magnetization is predicted to obey the universal scaling law (assuming $J_{\perp}/J_{\parallel} \gg 1$) that may be written as

$$\frac{M(H, T)}{M_s} = \sqrt{2k_B T/J_{\parallel}} \mathcal{M}(g\mu_B[H - H_{c1}]/k_B T),$$

$$1 - \frac{M(H, T)}{M_s} = \sqrt{2k_B T/J_{\parallel}} \mathcal{M}(g\mu_B[H_{c2} - H]/k_B T),$$

where the universal function \mathcal{M} is the fermion density [3]. This theoretically predicted scaling behavior is compared to the data in Fig. 4, where the agreement is impressive. It is important to stress that the scaling shown in Fig. 4

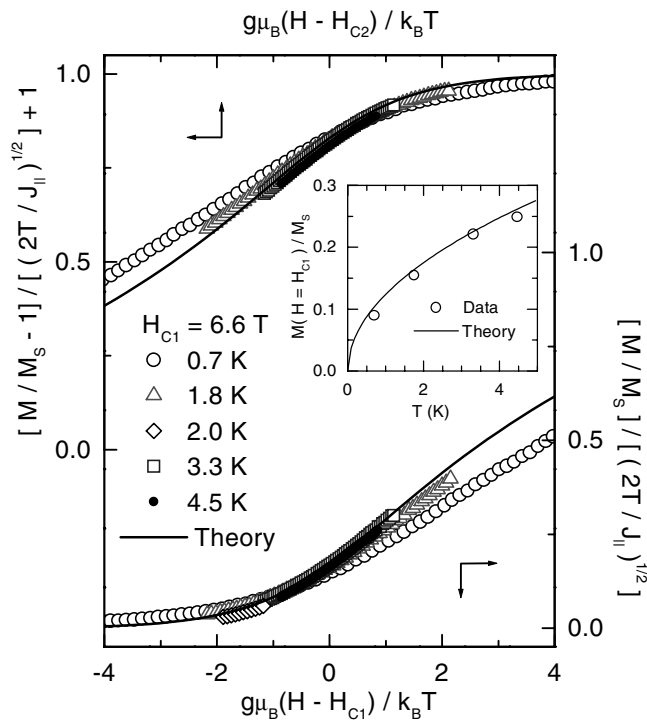


FIG. 4. The scaled data in the vicinity of H_{c1} and H_{c2} . The solid lines are the predictions of the theory when H_{c1} is fixed. The inset shows the $T^{1/2}$ scaling behavior at H_{c1} .

has been theoretically predicted [3] and is not a result of extracting scaling variables on the basis of the data [12]. In an isolated spin ladder, scaling is expected at the lowest temperatures, $T \lesssim J_{||}$. A deviation from scaling is observed for $T = 0.7$ K, which suggests that other weak interactions, such as J_F or J' , may begin to have a subtle influence, while the data up to 4.47 K appear to obey the scaling theory. The $T^{1/2}$ scaling of the magnetization at the critical point $H = H_{c1}$, Fig. 4, is further evidence that BPCB is a two-leg spin ladder with $J' \ll J_{||}$ [33].

In summary, analysis of $M(H \leq 30$ T, $T \geq 0.7$ K) has allowed us to identify BPCB as a two-leg $S = 1/2$ spin ladder in the strong-coupling limit, $J_{\perp}/J_{||} \sim 3.5$. A single set of exchange constants, $J_{\perp} = 13.3$ K and $J_{||} = 3.8$ K, are able to accurately describe all of the data. The $M(H \approx H_{c1}$ or H_{c2} , 1 K $< T < 4.5$ K) data exhibit scaling behavior in the universality class of the 1D dilute Bose gas transition [2,3]. Although we have considered the potential existence of additional exchange interactions J_F and J' , effects arising from these parameters are not prominent in the present data. However, since subtle differences arise between the theoretical predictions and the data at the lowest temperature, additional perturbing interactions may be present.

We have enjoyed input from many colleagues, including J.H. Barry, A. Feher, M. Orendáč, A. Orendáčova,

F. Mila, and A. Yashenkin. We thank G. Chaboussant for sending Ref. [8]. This work was supported, in part, by the NSF through DMR-9704225 (B.C.W. and M.W.M.), DMR-9357474 (V.N.K.), the NHMFL via DMR-9527035, DMR-9900855 (D.R.T. and co-workers), and by the State of Florida. Oak Ridge National Laboratory is managed for the DOE by UT-Battelle, LLC, under Contract No. DE-AC05-00OR22725.

- [1] E. Dagotto, Rep. Prog. Phys. **62**, 1525 (1999).
- [2] S. Sachdev, Science **288**, 475 (2000); *Quantum Phase Transitions* (Cambridge University Press, Cambridge, 1999).
- [3] S. Sachdev, T. Senthil, and R. Shankar, Phys. Rev. B **50**, 258 (1994).
- [4] B. Chiari *et al.*, Inorg. Chem. **29**, 1172 (1990).
- [5] P.R. Hammar and D.H. Reich, J. Appl. Phys. **79**, 5392 (1996).
- [6] C. A. Hayward, D. Poilblanc, and L. P. Lévy, Phys. Rev. B **54**, R12 649 (1996).
- [7] G. Chaboussant *et al.*, Phys. Rev. B **55**, 3046 (1997).
- [8] G. Chaboussant, Ph.D. thesis, Université Joseph Fourier, Grenoble, 1997 (unpublished).
- [9] Zheng Weihong, R. R. P. Singh, and J. Oitmaa, Phys. Rev. B **55**, 8052 (1997).
- [10] G. Chaboussant *et al.*, Phys. Rev. Lett. **79**, 925 (1997).
- [11] G. Chaboussant *et al.*, Phys. Rev. Lett. **80**, 2713 (1998).
- [12] G. Chaboussant *et al.*, Eur. Phys. J. B **6**, 167 (1998).
- [13] P.R. Hammar *et al.*, Phys. Rev. B **57**, 7846 (1998).
- [14] N. Elstner and R. R. P. Singh, Phys. Rev. B **58**, 11 484 (1998).
- [15] R. Calemczuk *et al.*, Eur. Phys. J. B **7**, 171 (1999).
- [16] H. Ohta *et al.*, J. Phys. Soc. Jpn. **68**, 732 (1999).
- [17] X. Wang and L. Yu, Phys. Rev. Lett. **84**, 5399 (2000).
- [18] H. Mayaffre *et al.*, Phys. Rev. Lett. **85**, 4795 (2000).
- [19] M. B. Stone *et al.*, cond-mat/0103023 (unpublished).
- [20] B. R. Patyal, B. L. Scott, and R. D. Willett, Phys. Rev. B **41**, 1657 (1990).
- [21] K. Totsuka, Phys. Rev. B **57**, 3454 (1998).
- [22] B. L. Brandt, D. W. Liu, and L. G. Rubin, Rev. Sci. Instrum. **70**, 104 (1999).
- [23] A complete analysis is given by B. C. Watson, Ph.D. thesis, University of Florida, 2000 (unpublished).
- [24] D. C. Johnston *et al.*, cond-mat/0001147 (unpublished).
- [25] M. Takahashi and M. Suzuki, Prog. Theor. Phys. **48**, 2187 (1972).
- [26] F. Mila, Eur. Phys. J. B **6**, 201 (1998).
- [27] M. Reigrotzki, H. Tsunetsugu, and T. M. Rice, J. Phys. Condens. Matter **6**, 9235 (1994).
- [28] H. Kageyama *et al.*, Phys. Rev. Lett. **82**, 3168 (1999).
- [29] W. Shiramura *et al.*, J. Phys. Soc. Jpn. **67**, 1548 (1998).
- [30] B. Kurniawan *et al.*, Phys. Rev. Lett. **82**, 1281 (1999).
- [31] A. M. Tselvik, Phys. Rev. B **42**, 10 499 (1990).
- [32] I. Affleck, Phys. Rev. B **43**, 3215 (1991).
- [33] T. Giamarchi and A. M. Tselvik, Phys. Rev. B **59**, 11 398 (1999).